CNN based Power System Transient Stability Margin and Voltage Stability Index Prediction

Karthikeyan Balasubramaniam,
Ganesh Kumar Venayagamoorthy
Real-Time Power and Intelligent Systems Laboratory
Holcombe Dept. of Elect. and Computer Engg.
Clemson University, Clemson, SC 29634
karthik_bala@ieee.org and gkumar@ieee.org

Neville Watson
Department of Electrical Engineering
University of Canterbury
Christchurch, New Zealand
neville.watson@canterbury.ac.nz

***Abstract*—Operators at electric grid control centers are faced with the task of making important decisions in real-time. With the plethora of data available it becomes important to extract information from the available data, based on which knowledge of system condition can be formed. This knowledge can then be used in decision making. Metrics such as transient stability margin (TSM) and voltage stability load index (VSLI) help in assessing the stability of the system. In this study, cellular neural network (CNN) based stability margin prediction system is developed in a distributed computing framework. The developed system not only extracts information from available data but also predicts the same, one step ahead of time. Moreover, the framework employed uses distributed computing and hence could be used on a large scale power system with a linear increase in computation time instead of an exponential increase. A reduced version of New Zealand's South Island power system is used as the test system to demonstrate the feasibility of CNNs for TSM and VSLI prediction.**

***Index Terms*—Cellular neural networks, dynamic security assessment, real-time monitoring, smart grid, transient stability margin, voltage stability load index.**

I. Introduction

As the demand for electrical energy increases, the existing infrastructure is being pushed closer to its limit. At the same time, integration of renewable energy sources introduces conditions of high uncertainty and high variability [1]. In recent years, opening up of transmission systems to non-utility members to export power to the grid has complicated operation and increased security risks [2]. Under these conditions operating electric grids in a reliable manner is a challenging task.

Reliable operation requires that certain key conditions are met. The two major aspects of stability are with respect to generator angular limit and voltage limit of buses. Generators in a power grid are distributed geographically and operate in parallel. This parallelism is governed by synchronous operation of generators i.e. operating at the same frequency. Once synchronism is lost, generators can no longer operate in unison and hence their output cannot be aggregated. Transient stability margin (TSM) gives the distance to that critical point at which generators lose synchronism. Various methods have been used in literature to obtain TSM. In [3]–[5] the authors use the energy function method to study TSM while in [6]–[8] the authors use a single machine infinite bus equivalent system.

In a similar manner, voltage instability and subsequent voltage collapse can occur when load at a particular bus is increased beyond a certain limit. This limit depends not only on the loading at the bus in question but also depends on loading elsewhere in the interconnected system. Reference [9] gives a scalar number to each load bus. The so called L-index is a number between 0 and 1 and indicates the proximity to voltage collapse. Reference [10] gives a simplified procedure used for L-index calculation. Recently, singular value decomposition (SVD) of phasor measurement unit (PMU) data has been used as an indicator. The method views physical power system as a power flow solver - taking time varying loads/injections as inputs, and producing PMU-measured angles and voltage magnitudes as outputs. By observing a time window of PMU measurements it can be seen that outputs vary much more dramatically when the system is highly stressed. Hence, one of the outputs of SVD based PMU processing algorithm serves as a real-time indicator of system stress, tracking a well-established voltage stability performance metric without the need for detailed network parameter values or state estimator results [11]. Comparison of existing methods is given in [12].

This paper presents a way to dynamically predict these two stability margins, a step ahead of time. More specifically in this paper, five cycles ahead of time on a 50 Hz system. This is accomplished by using predictive modeling. Cellular neural networks (CNNs) is used for predictive modeling. Cellular neural networks have been used in literature for predictive modeling of power systems. References [13], [14] use CNNs to predict power system state variables. CNNs provide a generic framework that can take advantage of distributed computing power. A major advantage considering the fact that power system is made up of tens of thousands of individual elements and to be of practical use any new methodology proposed should be scalable.

The remaining sections of this paper are as follows. An overview of the topics covered in this paper is presented in Section II. In Section III, development of continuous stability limit prediction system is discussed in detail. In Section IV,

This work is supported by the National Science Foundation (NSF) of the United States, under grants CAREER ECCS 1231820, EFRI 1238097, ECCS 1232070 and RAPID 1216298. Any opinions, findings, and conclusions or recommendations expressed in this material are those of the author(s) and do not necessarily reflect the views of National Science Foundation.

978-1-4673-6002-9/13/$31.00 ©2013 IEEE

results are presented and discussed. Conclusions are drawn and future work is discussed in Section V.

II. Overview of Concepts and Test System

A. An Overview on Neural Networks

Neural networks (NNs) are known as universal function approximators. NNs can learn system dynamics from historical data without the need for a detailed system model. Detailed mathematical model for a lot of practical applications is either unavailable or too complex. This makes NNs a suitable candidate for the problem at hand. By mapping the input-output relationships of state variables NNs can effectively capture the dynamics and hence can be used to predict how these state variables will evolve over time given the control signal. The problem can be generalized as,

$$x(t+1) = f(x(t), u(t)) \tag{1}$$

Where x is the state variable and u is the control signal. In essence, it is comparable to a time domain simulation with the difference being the time step used. Differential algebraic equations used to describe the dynamics of power systems are stiff and hence to ensure reliable results very small time steps in the order of microseconds are used. Such step sizes ensure that the linear approximation is valid and numerical integration is carried out to find successive points and hence evolution of state variables over time. In the following sections it is demonstrated that NNs with time steps in the order of 100 milliseconds can provide results with the desired accuracy.

B. Distributed Computation using CNN

The advantages of NNs were presented in the previous sub-section. However, there are certain drawbacks that need to be addressed. The drawback has to do with the scalability issues with a neural network for large systems. Electric grid is a highly interconnected system with tens of thousands of buses and the number of state variables could easily run into several hundred thousand. To be of any practical use, the developed system must be capable of handling a large number of state variables in multiple timescales starting at milliseconds. Traditional NN architectures would require large amount of time to carry out a prediction and also because the number of connections are large, the dynamics to be learnt become more complex and hence NN performance could deteriorate.

Cellular neural networks (CNN) [14], [15] on the other hand make scaling linear by breaking down the problem into several sub-problems. This breakdown can be achieved with domain knowledge, for example although every variable in a power system influences other variables it is usually only a subset of these variables that have a pronounced effect.

As the size of the network increases, the difference in the number of weights in cellular neural networks and conventional neural network architecture increases. This can be best illustrated from the following table. Table I shows that scaling is not linear in the conventional multilayer perceptron (MLP) architecture, where as it is linear in cellular MLP architecture. Furthermore, cellular architecture is inherently parallel, making it an even more exciting prospect as the problem can be parallelized. Each of the cells can be made to run on a processor in a high performance computing cluster, thereby making use of the parallel and distributed architecture of cellular neural networks.

Table I: COMPARISON BETWEEN CELLULAR MLP AND EQUIVALENT SINGLE MLP

Test System	Equivalent single MLP	Cellular MLP
12-bus (4 Generator)	n=16,m=32,r=4 No of weights=640	n=6,m=12,r=1, N=4 No of weights= 336
68-bus (16 Generator)	n=64,m=128,r=16 No of weights=10240	n=6,m=12,r=1,N=16 No of weights=1344

It is to be noted that the concept of CNN is a framework, meaning the computational unit could be neural network or a mathematical model that could accomplish the required task. In this study, a feedforward neural network is used, more specifically, MLP with standard back-propagation as the learning algorithm [16]. It is also possible to use heterogeneous computational networks, i.e. one could use a MLP, recurrent neural network (RNN), simultaneous recurrent neural network (SRN) etc. as cells in a CNN. One could go a step further and use NNs for a part of the cells in CNN and use mathematical models for the remaining cells.

C. Test System

In this study, New Zealand's South Island (SI) equivalent electric grid is used. The South Island's electric grid is an interesting test case because the Alpine fault runs almost the entire length of Southern Island and presents a suitable test scenario where equipment failure due to earthquakes can be simulated. An equivalent South Island system as shown in Fig. 1 is modeled in RSCAD [17], the front-end for real-time digital simulator (RTDS). There are seven separate generating stations where each station has a number of generators. An aggregated model for generating stations is used i.e. all the generating units in a generating station are aggregated to form an equivalent unit. There are 19 buses, seven loads and 22 transmission lines. All the lines are rated at 220 kV.

The Clyde generating station is located right on fault line. Here, fault line refers to a line that stretches along the ground where a fault is likely to happen i.e. an earthquake prone zone. The system is taken from [18] and modified to include Clyde generating station. The system is modeled with full transient dynamics.

III. Continuous Stability Limit Prediction System

Stability limit predictions are carried out on distributed computing framework as shown in Figs. 2 and 3. Each block, referred to as a cell in the CNN is a computing unit, which models the behavior of a power system component [13]. For example, each cell in the transient stability margin prediction layer represents a generator. These cells transfer information between each other leading to a decentralized learning framework [14]. The details of implementation for each layer are discussed in the following sub-sections.

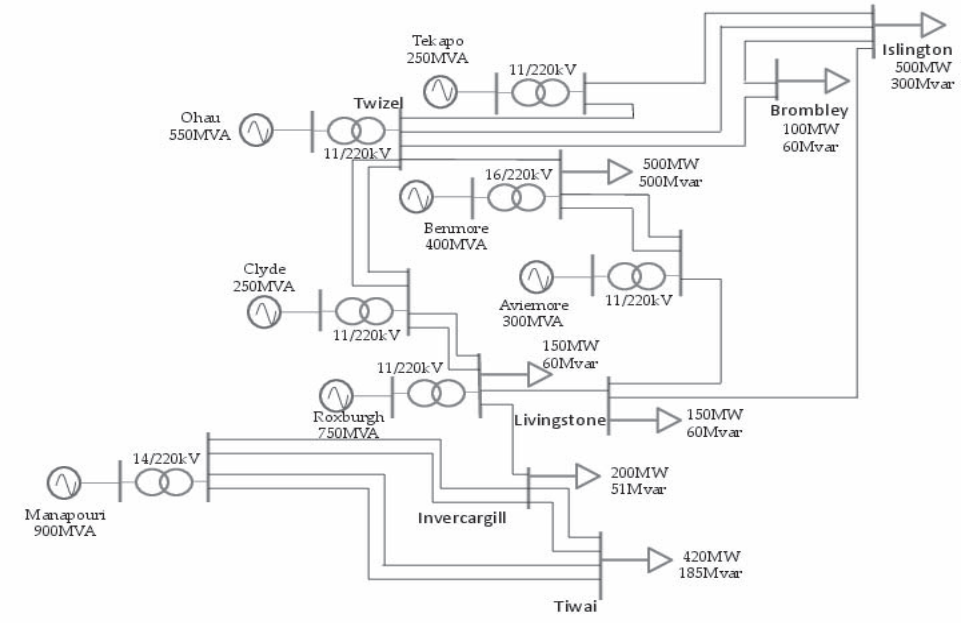

Figure 1: One line diagram of South Island equivalent system

A. Transient Stability Margin

A brief discussion of synchronous machines and angle stability is first presented and then transient stability margin is discussed. Synchronous machines have field and armature winding, generally field winding is on the rotor while armature winding is on the stator. Field winding is energized by DC current. The rotor is coupled to the prime mover (turbine) and when the rotor is driven by prime mover the rotating magnetic fields of the field winding induces alternating voltage in the three-phases of the stator winding [19].

Frequency of induced magnetic field depends on the frequency of the rotor. In other words, both rotor and stator fields are synchronized. Electromagnetic torque is produced because of the tendency of stator and rotor magnetic fields to align themselves. In a generator, this torque opposes the rotation of the rotor and hence mechanical torque must be provided to sustain rotation. The equilibrium between mechanical torque input and electrical power output maintains a constant rotor speed. Several such synchronous machines are operated in parallel in power systems. Hence, all the interconnected machines must be in synchronism.

Power transfer is a highly nonlinear relationship and it depends on the rotor angle deviation between machines. Until a certain value of angular separation the power transferred increases and beyond that point power transfer decreases. This angular separation results in inherent stability property of synchronous machines. Imagine a scenario where one generator is running faster than normal, this generator is connected to other generators in the system which are running at normal speed. Since increase in angular separation results in increased power transfer, some of the load of the slower running machines is transferred to faster running machine and gradually a steady state operating point will be reached.

Table II: INPUT-OUTPUT MAPPING FOR TRANSIENT STABILITY LAYER

Generator	Input (self)	Input (neighbors)	Control Input (PRBS/pss+ vref-vt)	Output
Aviemore	$\delta_{avi}(t, t-1, t-2)$	$\delta_{ben}(t)$	$U_{avi}(t)$	$\delta_{avi}(t+1)$
Benmore	$\delta_{ben}(t, t-1, t-2)$	$\delta_{avi}(t)$, $\delta_{rox}(t)$	$U_{ben}(t)$	$\delta_{ben}(t+1)$
Clyde	$\delta_{cly}(t, t-1, t-2)$	$\delta_{man}(t)$, $\delta_{rox}(t)$	$U_{cly}(t)$	$\delta_{cly}(t+1)$
Manapouri	$\delta_{man}(t, t-1, t-2)$	$\delta_{cly}(t)$, $\delta_{rox}(t)$	$U_{man}(t)$	$\delta_{man}(t+1)$
Ohau	$\delta_{oha}(t, t-1, t-2)$	$\delta_{rox}(t)$, $\delta_{tek}(t)$	$U_{oha}(t)$	$\delta_{oha}(t+1)$
Roxburgh	$\delta_{rox}(t, t-1, t-2)$	$\delta_{man}(t)$, $\delta_{ben}(t)$, $\delta_{oha}(t)$	$U_{rox}(t)$	$\delta_{rox}(t+1)$
Tekapo	$\delta_{tek}(t, t-1, t-2)$	$\delta_{oha}(t)$	$U_{tek}(t)$	$\delta_{tek}(t+1)$

However, if the angular separation between machines goes beyond a certain point the reverse happens and this leads to instability. Transient stability margin gives the distance to that critical point. The transient stability margin is calculated for each machine by finding the angular separation between each generator and an equivalent model of all generators, using the center of inertia (COI) method. It is formulated as,

$$\delta_{COI} = \frac{\sum_{i=1}^{n} H_i \delta_i}{\sum_{i=1}^{n} H_i} \tag{2}$$

$$TSM_i = \delta_i - \delta_{COI} \tag{3}$$

In order to predict TSM, transient stability margin prediction layer predicts rotor angle deviation and from that TSM is calculated mathematically as defined in (3) [20]. The TSM prediction problem is formulated as given in (4) where $\triangle V_{ref,i}$ is the difference between reference voltage magnitude and actual voltage magnitude of generator, δ_i is the rotor angle of the generator and δ_n is rotor angle of neighboring generator.

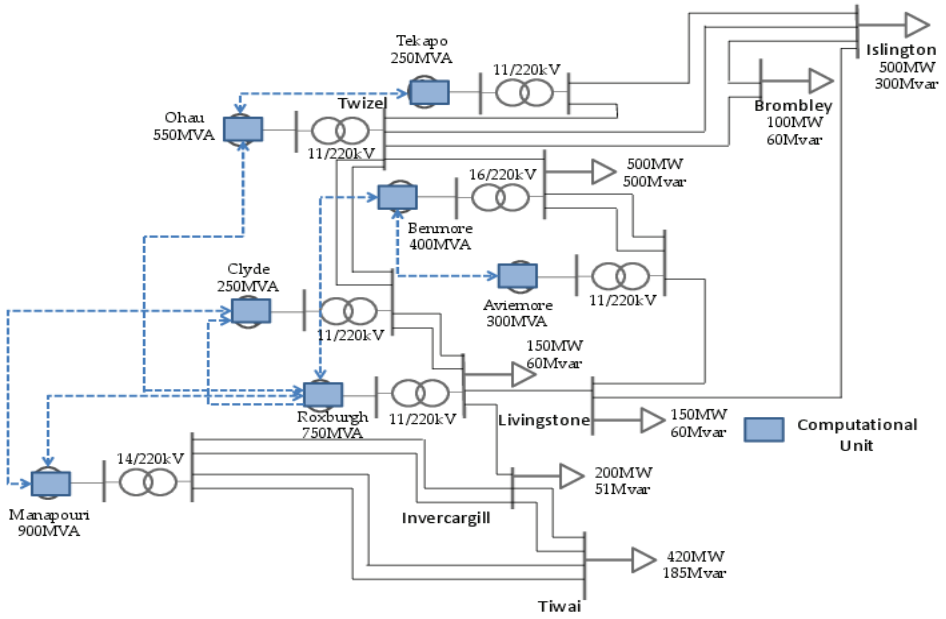

Figure 2: Transient stability margin prediction scheme is shown. Computational units are superimposed on top of one line diagram to show how spatial dynamics are captured. Information exchange is shown as directed arrows.

Neighbors are defined in Fig. 2 and formulation is given in Table II.

$$\hat{\delta}_i(t+n\triangle t) = f_\delta(\delta_i(t-m\triangle t), \delta_n(t), \triangle V_{ref,i}(t)) \quad (4)$$

Here, m takes the value of 0 to 2 i.e. value of a variable at time t, $t-1$, $t-2$ are used. In this paper, n is 1 and $\triangle t$ is $100\,ms$ or five cycles.

B. Voltage Stability Load Index

Voltage stability can be defined as the ability of the power system to maintain acceptable voltage levels during normal conditions and during disturbances [19]. One of the main factors contributing to voltage instability and subsequently voltage collapse is the inability of power system to supply the required amount of reactive power. Voltage instability could be viewed as negative relationship between voltage at a bus and reactive power injection at that bus. In other words, a system is said to be stable with respect to voltage, if an increase in reactive power injection at that bus results in an increase in voltage. On the other hand when there is a negative relationship i.e. an increase in reactive power injection results in a decrease in voltage can be viewed as voltage instability.

Voltage instability is a local phenomenon, however voltage collapse is a complex phenomenon and occurs as a result of sequence of events [19]. Many studies have been carried out to determine voltage stability indices in order to facilitate the necessary control actions to preclude eminent instability and thereby improving voltage stability in a power system [21]. There are various methods of determining voltage stability load index (VSLI) in literature. Singularity of the Jacobian of power flow equations have been used as a test for onset of voltage collapse [9], [22].

The one used in this study is based on a function of no-load and load voltage. It is difficult to calculate voltage stability load index dynamically because the no-load voltage is a function of loading at different buses. At any given time, loading at buses are going to vary and hence a look up table approach is not possible as the number of combinations are large. Also, calculating no-load voltage requires power-flow calculations and this is difficult to obtain in a short span of time. Voltage stability load index can be calculated with the following formula as given in [23],

$$VSLI = \frac{4(V_0 V_L cos(\theta_0 - \theta_L) - V_L^2 cos^2(\theta_0 - \theta_L))}{V_0^2} \quad (5)$$

V_L and θ_L are the voltage magnitude and angle of load bus while V_0 and θ_0 are the no-load voltage magnitude and angle respectively. Equation (5) results in a numeric value between 0 and 1. A value of 1 represents voltage collapse point. Hence, by calculating VSLI, distance to voltage collapse point can be identified and preventive control actions, if required, could be taken. In this paper, VSLI at a given bus is predicted in the following way,

$$\hat{VSLI}_i(t+n\triangle t) = f_{vsli}(V_i(t-m\triangle t), \theta_i(t-m\triangle t)) \quad (6)$$

Data for training is obtained through continuation power-flow. Continuation power-flow remains well-conditioned at and around the critical point [24] and hence data from no-load to critical loading condition can be obtained.

IV. Results and Discussion

A. System Identification

As discussed before, neural networks can learn system dynamics from historical input-output data. However, the input-output data should be such that the dynamics of the system are

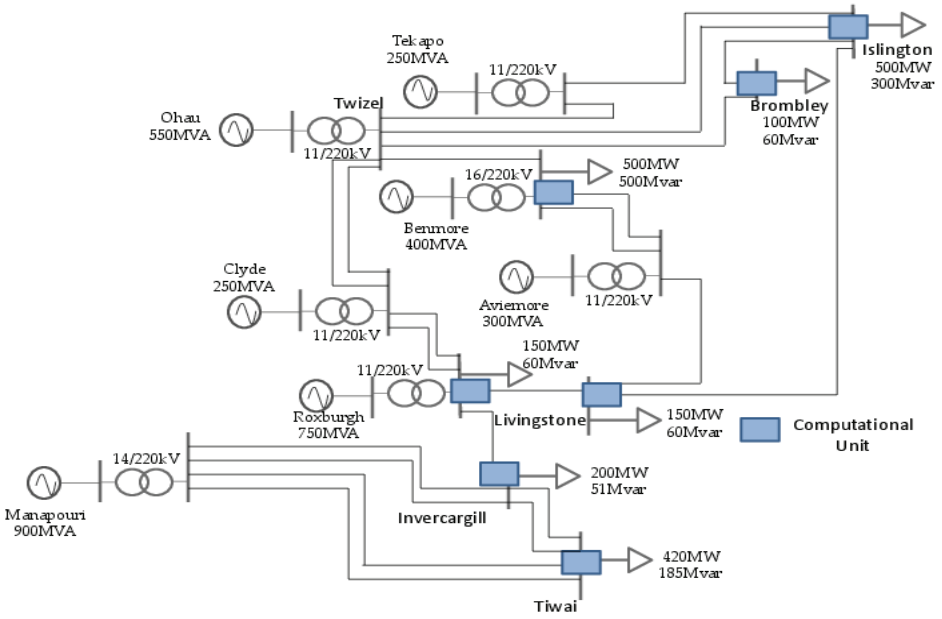

Figure 3: Each block represents a cell. Seven different cells predict voltage stability load index at seven different load buses.

captured over a wide range. To this end there are two different approaches, the first of these approaches is by using what is known as pseudorandom binary signal (PRBS). PRBS is injected to the automatic voltage regulator (AVR) of generator. The AVR then responds to these signals thereby causing a disturbance in the system. The resulting data is captured and a subset of the data is kept for testing while the remaining data is used for training. This technique is called forced training. The second approach is to do natural training [25]. In natural training, a sudden change in system dynamics, such as a fault is simulated and the resulting data is captured and used for training and testing. The testing results are presented in Figs. 4 and 5.

B. Metrics

Evaluating the goodness of fit by means of a metric is difficult. For example, mean square error (MSE) generally gives a good value if the variable is between 0 and 1. For example, take the case of speed deviation prediction, when the actual value is .001, and the predicted value is .002. Even though the value is off by 100% one would still get an MSE of 10^{-6}, which is misleading. In the event that the values are normalized between 0 and 1, the values closer to 0 will have the same trend as discussed above. Root mean square error (RMSE) is better than MSE in this aspect. Another metric, absolute relative error (ARE) is also used in literature.

$$MSE = \frac{\sum_{i=1}^{N}(actual_i - predicted_i)^2}{N} \tag{7}$$

$$RMSE = \sqrt{\frac{\sum_{i=1}^{N}(actual_i - predicted_i)^2}{N}} \tag{8}$$

$$ARE = \frac{|actual - predicted|}{|actual|} \tag{9}$$

ARE also suffers from scaling issues. If actual values instead of normalized values are used, the results might be misleading. Let us consider a quantity that varies between 300 and 400. When normalized between a value of 0 and 1, a value of 330 corresponds to 0.3 and let's say the predicted value is 333 i.e. 0.33 on the normalized scale. Applying the formula given in (9), one would get an ARE of 0.1 or 10% whereas the same measure on actual scale would give 0.0091 or 0.91%. To give a fair indication as to how well the developed CNN based system performs, all three metrics are presented so that negative aspects of one metric can be compensated by the other. Table III gives the results for VSLI and TSM layer based on average performance of all cells in each layer. Results presented are for pseudorandom binary signal injection in the case of TSM layer and from continuation power-flow in the case of VSLI layer.

Table III: METRICS FOR VSLI AND TSM LAYER

Layer	MSE	RMSE	ARE
VSLI	1.48×10^{-3}	3.85×10^{-2}	8.27×10^{-2}
TSM	5.15×10^{-4}	2.27×10^{-2}	4.92×10^{-2}

C. Discussion on Results

Results are presented for forced and natural training. The results give a visual indication for the goodness of fit. Good tracking performance for both the prediction layers is observed. Transient stability margin is the rotor angle difference between a particular generator and a reference. The method used in this paper to find the equivalent reference generator is called center of inertia. Figs. 4 (a) and (b) shows actual and predicted values of angular separation between rotor angle of generator at Tekapo and the equivalent generator calculated using center of inertia method. In Fig. 4 (a) the system is perturbed by PRBS injection and in Fig. 4 (b) the operating point of system is changed from base case.

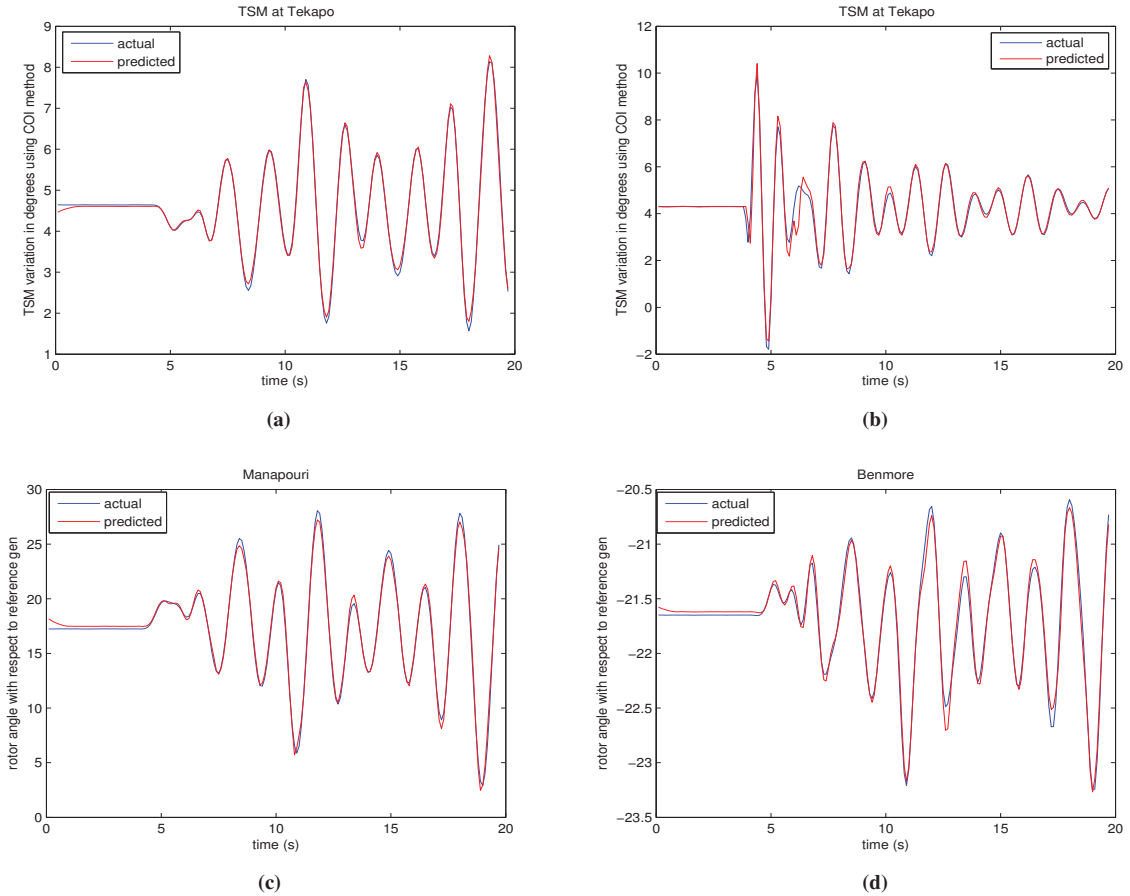

Figure 4: (a) Transient stability margin of generator at Tekapo when subjected to PRBS injections. (b) TSM variation at Tekapo due to 6-cycle three phase to ground fault at Islington. (c) Rotor angle deviation prediction for generator at Manapouri when subjected to PRBS injection. (d) Rotor angle deviation prediction for generator at Benmore when subjected to PRBS injection.

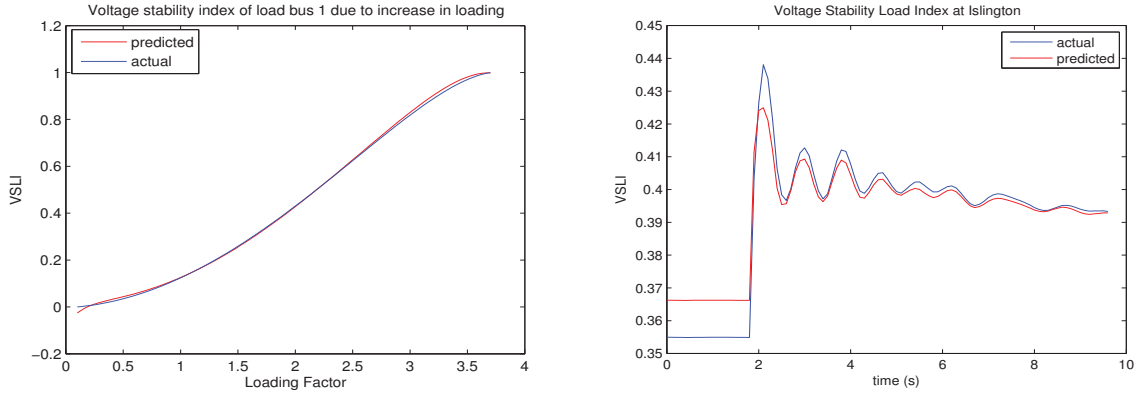

Figure 5: (a) Voltage stability load index variation at Invercargill as a result of increased loading at Invercargill. Load is increased from base load to the point of voltage collapse. (b) VSLI variation at Islington due to 25% increase in real power loading from base case.

Loading at Roxburgh is changed from base case loading of 150 MW and 60 Mvar to 200 MW and 60 Mvar. Under steady state in the new operating condition a six cycle 3-phase to ground fault is applied. Figs. 4 (c) and (d) display the rotor angle deviation of Manapouri and Benmore generating stations with respect to Roxburgh generator, which is the reference generator for the system. Fig. 5 (a) is the result from continuation power flow where loading factor is increased till the point of voltage collapse. In Fig. 5 (b), a sudden increase in loading at Islington i.e. 25% increase in active power consumption from base case results in an increase in VSLI. Load increase is applied at 1.8 seconds. In this particular figure, in order to prove tracking performance of VSLI layer, actual and predicted values are both plotted for time t. The reason being, a load change cannot be predicted ahead of time and hence if VSLI for $t+1$ were to be predicted the change at that particular point when load is increased would be missed.

Hence, to illustrate tracking performance during sharp changes in operating conditions, prediction is shown for t instead of $t + 1$. Results shown indicates slight mismatch between actual and predicted values of VSLI at both steady-state and during transients. The reason being, as stated in the previous section, the no-load voltage magnitude and angle are not available and CNN is trained under various operating conditions in order to facilitate learning without having the values of missing components. However, after having trained under several different operating conditions, an optimized value for no-load voltage magnitude and theta is ascertained by CNN that gives least error when applied under various conditions.

The relationship between no-load voltage magnitude and angle at a bus is a function of load variation across the system. Thus, unless system wide loading conditions are explicitly provided it would be impossible for the CNN to learn the required functional relationship. Hence, with the limitations in mind, the problem is formulated in such a way that VSLI can be predicted purely as a function of voltage profile at a given load bus. Hence, there is a slight variation between actual and predicted values at steady state and during transients.

V. Conclusions and Future Work

Identification of stability margin is essential for secure and reliable operation of electric grid. This paper is aimed at making sense of power system data by transforming data to information which could then be used to form knowledge of system conditions, based on which control decisions can be made. To this end, a distributed framework for predicting stability margin is presented. Voltage and transient stability indices are predicted using cellular neural network architecture. The use of cellular architecture makes it possible to use parallel and distributed computing framework. This is an important aspect because power system is highly interconnected with tens of thousands of state variables. To be able to handle a system of such size in acceptable amount of computing time is a challenging task and this study presents a way to handle large amounts of data.

Feasibility of using CNN framework for predicting stability indices is demonstrated using an equivalent New Zealand South Island system. Future work is aimed at achieving multi-step predictions. To do so with acceptable computational time, the algorithm will be implemented on high performance computing cluster. Longer lead times would help to foresee an imminent blackout based on which anticipatory actions can be executed.

References

[1] J. Liang, G. K. Venayagamoorthy, and R. G. Harley, "Wide-area measurement based dynamic stochastic optimal power flow control for smart grids with high variability and uncertainty," *IEEE Transactions on Smart Grid*, vol. 3, no. 1, pp. 59–69, 2012.

[2] A. J. Wood and B. Wollenberg, *Power generation operation & control*. John Wiley & Sons, 1996, ISBN-13: 978-0471586999.

[3] A. A. Fouad and V. Vittal, *Power system transient stability analysis using the transient energy function method*. Prentice Hall, 1991, ISBN-13: 978-0136826750.

[4] V. Vittal, G. M. Prabhu, and S. L. Lim, "A parallel computer implementation of power system transient stability assessment using the transient energy function method," *IEEE Transactions on Power Systems*, vol. 6, no. 1, pp. 167–173, 1991.

[5] Y. Dong and H. R. Pota, "Transient stability margin prediction using equal-area criterion," in *IEE Generation, Transmission and Distribution Proceedings*, vol. 140, no. 2. IEE, 1993, pp. 96–104.

[6] M. Pavella, "Generalized one-machine equivalents in transient stability studies," *Power Engineering Review, IEEE*, vol. 18, no. 1, pp. 50–52, 1998.

[7] T. C. Juarez, R. Castellanos, and A. R. Messina, "Analysis of inter-area oscillations using timevarying one-machine infinite bus equivalents," in *Power Engineering Society General Meeting,*. IEEE, 2005, pp. 923–930.

[8] T. C. Juarez, A. R. Messina, and D. Ruiz-Vega, "Analysis and control of the inter-area mode phenomenon using selective one-machine infinite bus dynamic equivalents," *Electric power systems research*, vol. 76, no. 4, pp. 180–193, 2006.

[9] P. Kessel and H. Glavitsch, "Estimating the voltage stability of a power system," *IEEE Transactions on Power Delivery*, vol. 1, no. 3, pp. 346–354, 1986.

[10] T. Q. Tuan, J. Fandino, N. Hadjsaid, J. C. Sabonnadiere, and H. Vu, "Emergency load shedding to avoid risks of voltage instability using indicators," *IEEE Transactions on Power Systems*, vol. 9, no. 1, pp. 341–351, 1994.

[11] T. Overbye, P. Sauer, C. DeMarco, B. Lesieutre, and M. Venkatasubramani, "Using pmu data to increase situational awareness," University of Illinois at Urbana-Champaign, University of Wisconsin-Madison, Washington State University, Tech. Rep., 2010.

[12] A. K. Sinha and D. Hazarika, "A comparative study of voltage stability indices in a power system," *International journal of electrical power & energy systems*, vol. 22, no. 8, pp. 589–596, 2000.

[13] K. Balasubramaniam, B. Luitel, and G. K. Venayagamoorthy, "A scalable wide area monitoring system using cellular neural networks," in *The International Joint Conference on Neural Networks (IJCNN)*. IEEE, June 10-15 2012, pp. 1–8.

[14] B. Luitel and G. K. Venayagamoorthy, "Decentralized asynchronous learning in cellular neural networks," *IEEE Transactions on Neural Networks and Learning Systems*, vol. 23, no. 11, pp. 1755–1766, 2012.

[15] L. O. Chua and L. Yang, "Cellular neural networks: Applications," *IEEE Transactions on Circuits and Systems*, vol. 35, no. 10, pp. 1273–1290, 1988.

[16] P. J. Werbos, "Backpropagation through time: what it does and how to do it," *Proceedings of the IEEE*, vol. 78, no. 10, pp. 1550–1560, 1990.

[17] RTDS, *Real time digital simulator tutorial manual (rscad version)*, RTDS Technologies, March 2008.

[18] J. Arrillaga and N. R. Watson, *Power systems electromagnetic transients simulation*. Institution of Electrical Engineers, 2002, ISBN-13: 978-0852961063.

[19] P. Kundur, N. J. Balu, and M. G. Lauby, *Power system stability and control*. McGraw-hill New York, 1994, ISBN-13: 978-0070359581.

[20] C. J. Tavora and O. J. M. Smith, "Characterization of equilibrium and stability in power systems," *IEEE Transactions on Power Apparatus and Systems*, no. 3, pp. 1127–1130, 1972.

[21] K. J. Makasa and G. K. Venayagamoorthy, "On-line voltage stability load index estimation based on pmu measurements," in *Power and Energy Society General Meeting,*. IEEE, 2011, pp. 1–6.

[22] B. M. Weedy and B. R. Cox, "Voltage stability of radial power links," *Proceedings of the Institution of Electrical Engineers*, vol. 115, no. 4, pp. 528–536, 1968.

[23] T. K. A. Rahman and G. B. Jasmon, "A new technique for voltage stability analysis in a power system and improved loadflow algorithm for distribution network," in *Proceedings of EMPD'95., International Conference on Energy Management and Power Delivery*, vol. 2. IEEE, 1995, pp. 714–719.

[24] V. Ajjarapu and C. Christy, "The continuation power flow: a tool for steady state voltage stability analysis," *IEEE Transactions on Power Systems*, vol. 7, no. 1, pp. 416–423, 1992.

[25] G. K. Venayagamoorthy and R. G. Harley, "A continually online trained neurocontroller for excitation and turbine control of a turbogenerator," *IEEE Transactions on Energy Conversion*, vol. 16, no. 3, pp. 261–269, 2001.